A NON-UNIFORM CORROSION MODEL AND MESO-SCALE FRACTURE MODELLING OF CONCRETE

Xun Xi[1, 2], Shangtong Yang[2*] and Chun-Qing Li[3]

[1] *School of Civil and Resource Engineering, University of Science and Technology Beijing, Beijing, 100083, China.*

[2] *Department of Civil and Environmental Engineering, University of Strathclyde, Glasgow, G1 1XJ, United Kingdom.*

[3] *School of Engineering, RMIT University, Melbourne, Vic 3001, Australia.*

ABSTRACT

Corrosion-induced concrete cracking is a significant durability problem for reinforced concrete structures. Considerable research has been carried out in the last few decades to understand and model the expansion mechanism of the corrosion products around the reinforcing bar and simulate the cracking behaviour of the concrete cover. In this paper, a new corrosion model based on non-uniform corrosion expansion is formulated and validated against experimental data. A meso-scale fracture model, consisting of aggregates, cement paste/mortar and ITZ, is established for the cases of both middle and side reinforcing bars. Under the developed corrosion and concrete fracture model, the cracking phenomena of the concrete cover are accurately simulated. It has been found that the non-uniform corrosion model can be used to express the realistic corrosion rust progression around the reinforcing bar, with the best accuracy. It has also been found that some microcracks occur before they are connected to form the dominating discrete crack which usually appears on the concrete surface. Moreover, the effects of the corrosion variables, as well as other key material and geometric parameters, on surface cracking of concrete are investigated.

Keywords: non-uniform corrosion, cohesive crack model, meso-scale, reinforced concrete structures, finite element method.

* Corresponding author. Tel: +44 141 548 3273. Email: shangtong.yang@strath.ac.uk.

1 INTRODUCTION

Reinforced concrete (RC) structures are widely used for civil structures and infrastructures, e.g., buildings, bridges, retaining walls and tunnels. Concrete are normally considered a durable material while corrosion of reinforcement has significant effects on the durability of RC structures. Cracks induced by corrosion destroy the integrity of concrete cover, reduce the reliability of concrete and lead to premature failure of RC structures and infrastructure. Worldwide, the maintenance and repair costs for corrosion-affected concrete infrastructure are estimated around $100 billion per annum [1]. With regard to serviceability and timely maintenance of the corrosion-affected RC structures and infrastructures, the engineers and/or asset managers need better informed decisions.

Over the past two decades, considerable research has been carried out in understanding and simulating the cracking mechanism of concrete cover induced by corrosion of reinforcement [2-8]. Andrade et al. [2] indicated that a negligible loss (e.g., 20 μm) of the cross-section of reinforcing bar could lead to a crack width of 0.05-0.1 mm, based on accelerated corrosion tests. Liu and Weyers [3] modelled the surface cracking time of concrete cover due to corrosion of reinforcement, taking the thickness of the "porous zone" around the steel/concrete interface into account. Bhargava et al. [5, 6] proposed models for predicting the time to cracking by considering the residual strength of cracked concrete and the stiffness reduction. Li et al. [8] developed an analytical model to calculate the crack width of concrete cover by assuming the cracks smeared in concrete and considering concrete as a quasi-brittle material. Among these existing studies, most are focused on uniform or general corrosion of the reinforcement.

Chlorides, as well as moisture and oxygen, diffuse into concrete and reach a threshold value at the surface of steel bar, before the passive layer on steel surface is destroyed and corrosion is initiated [9]. However, it is rare to have a uniform corrosion around the reinforcing bar, due to different amount of chlorides, moisture and oxygen that are available on different sides of the reinforcement; for example, the side of a reinforcing bar facing concrete cover should have more sources to advance corrosion and hence more corrosion products accumulated on this side. Recently, many researchers have started to model the cracking of concrete cover induced by non-uniform corrosion of reinforcement. González et al. [10] perhaps first compared the depth of pitting corrosion penetration on steel bar with the depth of general corrosion and found that the maximum penetration of pitting corrosion on the steel bar is equivalent to about three to sixteen times of the penetration of general corrosion. Jang and Oh [11] extended the experimental results in [10] and designed a factor for the ratio of the maximum thickness of non-uniform corrosion layer to the thickness of uniform corrosion layer to express the non-uniform corrosion. Moreover, some researchers postulated corrosion products followed a linear decrease distribution along the circle of steel bar [12, 13]. Pan and Lu [14] proposed a non-linear corrosion model with a quadratic expansion function to model the cracking of concrete induced by non-uniform corrosion. Further, Yuan and Ji [15] conducted corrosion tests on RC samples by using artificial environmental chamber and found the corrosion products distribution around the reinforcement is in a semi-elliptical shape. Based on the semi-elliptical assumption, Yang et al. [16] proposed an analytical model to calculate the time to cracking of concrete cover and Xi and Yang [17] developed a numerical model to investigate cover cracking caused by corrosion of multiple reinforcing bars. In addition, Zhao et al. [18-21] carried out corrosion tests on RC samples and proposed a Gaussian non-uniform corrosion model to quantitatively define the corrosion products distribution. Tran et al. [22] and Qiao et al. [23] proposed a non-uniform corrosion model by considering uniform corrosion for part of rebar and no corrosion for the other part, according to their results of experiments.

Once corrosion boundary model is established, the cracking of concrete caused by corrosion of reinforcement can be simulated. Jang and Oh [11] simulated the stress to cracking of concrete based on the linear decrease non-uniform corrosion model and Mohr-Coulomb failure model. Zhao et al. [18] modelled the crack patterns of concrete based on Gaussian non-uniform corrosion model and smeared crack model for concrete. Zhang et al. [24] employed damage plasticity model to simulate the crack propagation of concrete based on elliptical non-uniform corrosion model. However, most studies considered concrete as a homogeneous material. The homogeneity assumption is only an approximation and, for more accurate prediction, concrete should be treated as a three-phase heterogeneous material at the mesoscale, consisting of cement paste/mortar, aggregate and interfacial transition zone (ITZ). It has been found that the mechanical behaviour of the ITZ between aggregate and cement paste has a significant effect on concrete strength and cracking prediction of concrete [25]. Du et al. [26] employed damage plasticity model to simulate the heterogeneous concrete cracking patterns under elliptical non-uniform corrosion model [15]. Branko et al. [13] and Chen et al. [12] built lattice models to simulate the time to cracking of heterogeneous concrete cover based on the linear decrease corrosion model proposed by Jang and Oh [11]. However, amongst these limited literatures on modelling heterogeneous cracking of concrete cover under non-uniform corrosion, almost none can predict discrete crack propagation and micro-cracking prior to the formation of the dominating discrete crack.

This paper attempts to develop a new rational model for concrete cover cracking induced by non-uniform corrosion of reinforcement. A novel non-uniform corrosion model is first formulated based on von Mises distribution and validated against test data. The corrosion model is then compared with existing non-uniform corrosion models in literatures, in terms of accuracy of fitting experimental data, and the merit of the developed corrosion model is discussed. Three parameters are modeled in the rust distribution function, i.e., the linear relationship to corrosion degree λ, the non-uniform coefficient k and the location of the maximum thickness of the corrosion rust layer μ. Under the expansion caused by corrosion of reinforcement, two heterogeneous discrete crack models are built to simulate the concrete cover cracking for the cases of middle rebar and corner rebar, respectively. The initial micro-cracking and the subsequent dominating discrete crack propagation, and the surface crack width development under various non-uniform corrosion coefficients are obtained. Moreover, the effects of thickness of the "porous zone" on cracking patterns and surface crack width are investigated.

2 EXISTING NON-UNIFORM CORROSION MODELS

In this section, all existing models on non-uniform corrosion rust distribution around the reinforcing bar are briefly summarized. The thickness of corrosion rust layer $T_{cl}(\theta)$ consists of two parts as shown in Figure 1(a), i.e., the corroded rebar with thickness $T_{co-st}(\theta)$ and the expansion displacement beyond the original rebar with thickness $T_d(\theta)$. Thus, $T_{cl}(\theta)$ can be expressed as follows:

$$T_{cl}(\theta) = T_{co-st}(\theta) + T_d(\theta) \tag{1}$$

For clarification, it should be mentioned that some of the existing non-uniform corrosion models are built based on the corrosion rust thickness distribution (i.e., $T_{cl}(\theta)$), e.g., [19, 22, 23], some based on the corroded steel bar (i.e., $T_{co-st}(\theta)$), e.g., [11, 15] and the others on the expansion displacement beyond the original bar (i.e., $T_d(\theta)$), e.g., [14].

According to the ratio α of rust expansion to corroded rebar, it can be approximately obtained as follows [27]:

$$T_{cl}(\theta) = \alpha \times T_{co-st}(\theta) \tag{2}$$

By substituting Equation (2) into Equation (1), $T_d(\theta)$ can be derived as follows:

$$T_d(\theta) = (\alpha - 1) \times T_{co-st}(\theta) \tag{3}$$

By substituting Equation (3) into Equation (2), $T_{cl}(\theta)$ can be obtained as follows:

$$T_{cl}(\theta) = \frac{\alpha}{\alpha - 1} \times T_d(\theta) \tag{4}$$

By Equations (2-4), the non-uniform corrosion models can be linked up.

2.1 Linear decrease corrosion model

Jang and Oh [11] assumed that the maximum thickness of corrosion is at the location of rebar nearest the concrete surface (i.e., θ=π) and the thickness of the corroded rebar $T_{co-st}(\theta)$ is linearly decreased from the outer region of the rebar. β is defined as the ratio of the maximum thickness of corroded rebar $T_{co-st,m}$ under non-uniform corrosion to the thickness of corroded rebar $T_{co-st,u}$ under uniform corrosion, given the same amount of corrosion products. As shown in Figure 1(b), the linear decrease corrosion model can be expressed as follows:

$$T_{co-st}(\theta) = \begin{cases} \beta \times T_{co-st,u}(1 - \dfrac{\pi - \theta}{\pi - \theta_0}), & \theta_0 < \theta < \pi \\ \beta \times T_{co-st,u}(1 - \dfrac{\theta - \pi}{\pi - \theta_0}), & \pi \le \theta < 2\pi - \theta_0 \\ 0, & 0 \le \theta \le \theta_0 \ \& \ 2\pi - \theta_0 < \theta \le 2\pi \end{cases} \tag{5}$$

Based on experimental results of González et al. [10] in which the value of β varies from about 4 to 8 in natural condition, three special cases, i.e., ($\beta = 2, \theta_0 = 0$), ($\beta = 4, \theta_0 = \frac{\pi}{2}$) and ($\beta = 8, \theta_0 = \frac{3\pi}{4}$) were employed to simulate non-uniform corrosion [11-13].

2.2 Quadratic function corrosion model

Pan and Lu [14] proposed a nonlinear semicircle expansion displacement model with a quadratic expansion function which can be expressed as follows:

$$T_d(\theta) = 4 \times T_{d,m} \left[\frac{(\theta - \frac{\pi}{2})}{\pi} - \left(\frac{\theta - \frac{\pi}{2}}{\pi} \right)^2 \right], \ \frac{\pi}{2} \le \theta \le \frac{3\pi}{2} \tag{6}$$

where $T_{d,m}$ is the maximum thickness of corrosion rust at $\theta = \pi$. The quadratic non-uniform corrosion model is illustrated in Figure 1(c).

2.3 Partly uniform corrosion model

Qiao et al. [23] proposed a simple non-uniform corrosion model considering only part of the rebar uniformly corroded, as shown in Figure 1(d). It can be expressed as follows:

$$T_{cl}(\theta) = T_{cl}^{'}, \qquad \theta_0 \le \theta \le 2\pi - \theta_0 \tag{7}$$

where $T_{cl}^{'}$ is the calculated thickness of corrosion layer to keep the amount of corrosion products of the partly non-uniform corrosion the same as that of whole uniform corrosion. θ_0 is the un-corroded angle of steel bar.

2.4 Elliptical corrosion model

Yuan and Ji [15] found the corrosion products distribution around the reinforcement is in a semi-elliptical shape and proposed an elliptical corroded rebar model as shown in Figure 1(e). It could be expressed as follows:

$$T_{co-st}(\theta) = R - \frac{R\cdot(R-T_{co-st,m})^2}{\sqrt{(R-T_{co-st,m})^2\cdot\sin^2\theta + (R)^2\cdot\cos^2\theta}}, \qquad \frac{\pi}{2}\le\theta\le\frac{3\pi}{2} \tag{8}$$

where R is the radius of steel bar and $T_{co-st,m}$ is the maximum thickness of corroded steel bar.

2.5 Gaussian corrosion model

Zhao et al. [18-21] carried out accelerated corrosion tests on RC samples and proposed a Gaussian non-uniform corrosion model which can be expressed as follows:

$$T_{cl}(\theta) = \frac{a_1}{a_2\sqrt{2\pi}} e^{-\left(\frac{\theta-u}{\sqrt{2}a_2}\right)^2} + a_3 \tag{9}$$

where u is the location of the maximum thickness of corrosion layer which could be set as π [21]. a_1 is the non-uniform coefficient of the corrosion layer, a_2 is the spread coefficient of the corrosion layer and a_3 is the uniform coefficient of corrosion layer. As shown in Figure 1(f), the function of corrosion products layer is displayed around the circumference of the original rebar in [18-21].

The existing five non-uniform corrosion models have been widely used to investigate the failure mechanism of RC structure covers under non-uniform corrosion assumption [10-16, 18, 20-24, 26, 28, 29]. For linear decrease model [11], it may be difficult to build the relationship between the parameters β and θ under the same amount of corrosion products. Therefore, existing studies only discussed three special cases for ($\beta=2, \theta_0=0$), ($\beta=4, \theta_0=\frac{\pi}{2}$) and ($\beta=8, \theta_0=\frac{3\pi}{4}$) [11-13]. For quardratic function model [14], the function considers only half of steel bar corroded. The partly uniform corrosion model is hypethetic and also the corrded angle is hard to determine. The elliptical corrosion model [15] is obtained from slices of corroded RC samples, which showed only half of the steel bar was corroded. However, the test results are limited and more data on a variety of corrosion degrees should be conducted to justify the elliptical model. For the Gaussian model, the non-uniform coefficient a_1 cannot accurately reflect the non-uniform level when the spread coefficient a_2 is larger than 1.5 [21].

3 A NEW CORROSION MODEL BASED ON VON MISES DISTRIBUTION

Von Mises distribution is a continuous probability distribution on a circle, which is the circular analogue of the normal distribution [30]. Von Mises distribution was first used to study deviations of atomic weights from integer values and has become an important function in the statistical theory [31].

By comparing all existing corrosion models, we have found the von Mises distribution could be ideal to express the shape of corrosion progression. The corrosion rust layer thickness $T_{cl}(\theta)$ can be formulated as follows:

$$T_{cl}(\theta) = \lambda \frac{e^{k\cos(\theta-\mu)}}{2\pi I_0(k)} \tag{10}$$

where λ is a fitting parameter, μ is the location where the maximum thickness of corrosion layer appears, $I_0(k)$ is the modified Bessel function of order 0 and k is the concentration coefficient to define the level of non-uniform. The parameters will be discussed later in details.

The total amount of corrosion products W can be expressed as follows:

$$W = W_m + W_s \tag{11}$$

where W_s is the amount of rust replacing the corroded steel with thickness $T_{co-st}(\theta)$ and W_m is the amount of rust expansion from the circumference of the origin rebar with thickness $T_d(\theta)$.

W_m can be obtained by an integration based on the radius of rebar:

$$W_m = \frac{1}{2}\int_0^{2\pi} (T_d(\theta) + R)^2 d\theta - \pi R^2 \tag{12}$$

Or,

$$W_m = \frac{1}{2}\int_0^{2\pi} (T_d(\theta)^2 + 2T_d R) d\theta \tag{13}$$

By neglecting the second order of small quantity, i.e., $T_d(\theta)^2$, W_m can be derived as follows:

$$W_m = \int_0^{2\pi} T_d(\theta) R d\theta \tag{14}$$

According to Equation (4), W_m can be rewritten as follows:

$$W_m = \int_0^{2\pi} \frac{\alpha - 1}{\alpha} T_{cl}(\theta) R d\theta \tag{15}$$

By substituting Equations (10) into Equation (15), it becomes:

$$W_m = \int_0^{2\pi} \frac{\alpha - 1}{\alpha} \lambda \frac{e^{k\cos(\theta - \mu)}}{2\pi I_0(k)} R d\theta \tag{16}$$

Further, it can be derived that:

$$W_m = \frac{\alpha - 1}{\alpha} R\lambda \int_0^{2\pi} \frac{e^{k\cos(\theta - \mu)}}{2\pi I_0(k)} d\theta \tag{17}$$

The integral part becomes the cumulative function of von Mises distribution in a whole circle and its value is 1. W_m can be expressed as follows:

$$W_m = \frac{\alpha - 1}{\alpha} R\lambda \tag{18}$$

The total amount of corrosion products W can be derived as follows:

$$W = \alpha W_s \tag{19}$$

By substituting Equations (19) into Equation (11), W can also be expressed as follows:

$$W = \frac{\alpha}{\alpha - 1} W_m \tag{20}$$

According to Equations (18) and (20), the total amount of corrosion products W can be expressed as follows:

$$W = R\lambda \tag{21}$$

It can be postulated that λ reflects directly the amount of corrosion products. It should be noted that the formula is accurate when the radius loss of corroded rebar is relatively small compared with the radius of origin rebar, which is the case in most engineering practice. It has been reported a very small corrosion degree, i.e., 12 μm radius loss of rebar, can cause a visible crack at surface of concrete cover [32]. Therefore, such a hypothesis of the von Mises model is well justified.

According to Equations (10) and (21), the corrosion layer thickness $T_{cl}(\theta)$ can be derived as follows:

$$T_{cl}(\theta) = \frac{W}{R} \times \frac{e^{k\cos(\theta-\mu)}}{2\pi I_0(k)} \tag{22}$$

The corrosion degree of reinforcement η can be expressed as follows:

$$\eta = \frac{W_s}{W_0} \times 100\% \tag{23}$$

where the W_0 is the original amount of the reinforcing steel.

According to Equations (19) and (22-23), the corrosion layer thickness $T_{cl}(\theta)$ can be written as a function of corrosion degree:

$$T_{cl}(\theta) = \alpha\pi R\eta \times \frac{e^{k\cos(\theta-\mu)}}{2\pi I_0(k)} \tag{24}$$

Therefore, the parameter λ has a linear relationship with corrosion degree η, and λ can be defined as the corrosion degree indicator.

4 VALIDATION, COMPARISONS AND PARAMETERS

To verify the proposed von Mises corrosion distribution model, test data on non-uniform corrosion development are searched and collected in a comprehensive manner. Figure 2 shows the regression analysis of the proposed von Mises model with the test data [15, 19, 23]. It should be mentioned that, the results from Qiao et al. [23] used corroded rebar thickness $T_{co-st}(\theta)$, while the data in other literature studies were based on the thickness of corrosion products layer $T_{cl}(\theta)$. The fitting parameters and R^2 (coefficient of determination) values for the test data are shown in Table1. It can be found that most values of R^2 are larger than 0.9. The R^2 of data 8 is 0.768, which is caused by significant crack width (i.e., 0.4 mm). It can be proved that, prior to occurrence of any significant crack, the von Mises model can predict the non-uniform corrosion progression very well.

The regression analysis of elliptical model [15], linear decrease model [11, 12], quadratic expansion model [14], Gaussian model [19] and the developed von Mises model with the test data in terms of $T_{cl}(\theta)$ are illustrated in Figure 3. It can be found the curves predicted by the developed von Mises model are closest to the experimental data. The average R^2 against the six groups of test data for the existing non-uniform models and the von Mises model are compared and shown in Figure 4. It can be seen that the von Mises model has the best accuracy in fitting with the experimental data. Meanwhile, the von Mises model can be regarded as a circular analogue of Gaussian model but leads to better prediction of corrosion rust distribution around the reinforcing bar. In addition, the von Mises model has less number of parameters in formulating the non-uniform corrosion rust progression and these parameters also have direct physical meanings.

As introduced in the experiments [15, 19, 23], the test data 4 and 6 were obtained from corrosion of corner rebar while the others were from corrosion of middle rebar. The polar coordinate system and the location of maximum thickness of corrosion layer in the experiments [15, 19, 23] are shown in Figure 5. From fitting results by von Mises model, the value of μ is near π, which means the von Mises model can describe the location of maximum thickness of corrosion layer well. As a corrosion model used to analyse cracking of concrete cover induced by non-uniform corrosion of reinforcement, the parameter μ can be set as π in the polar coordinate system.

In the von Mises distribution k is the concentration coefficient and the smaller the k is, the distribution will be more close to uniform. From the fitting results with the test data, the value of k varies from 0.555 to 3.362. To investigate the effect of k on corrosion layer distribution in the von Mises corrosion model, the corrosion layer distribution under four values of k are produced and plotted in Figure 6. It should be noted that the right figures in Figure 6 show the front of the corrosion layer based on a circle representing the original rebar, not the expansion displacements of corrosion products. When k is zero, the corrosion layer thickness $T_{cl}(\theta)$ becomes a constant value and the von Mises corrosion model describes uniform corrosion. Therefore, $k=0$ is a special case which represents uniform corrosion while all other values of k (must be positive) define non-uniform corrosion.

In real corrosion propagation process, the non-uniform coefficient k may not be a constant but varying along time. There is very limited experimental and observational data available which cannot warrant a thorough understanding and elaboration about k. However, in this study, it has been found that for most existing data larger value of λ leads to smaller k. Moreover, it is considered that when corrosion progresses, the non-uniform coefficient will be smaller and smaller, i.e. the corrosion will become more close to uniform. Nonetheless, it has not been proved yet and hard to predict the varying value of k under different corrosion degrees. The value of k may be related to chloride content, geometry of RC structures, corrosion degree and surface crack of concrete. As chlorides, moisture and oxygen diffuse into concrete, a small part of rebar near concrete cover first corrodes. The rusts gradually form which fill in the voids around steel/concrete interface and expand outwards. At this moment, the non-uniform coefficient k can be large. With the corrosion propagation, more regions of rebar start to corrode and more microcell corrosion forms. The non-uniform coefficient k will then decrease. In particular, after crack penetrates the concrete cover and the chloride and oxygen can subsequently reach the rebar directly, the rebar perhaps corrode almost homogeneously around its whole circumference. Having said this, it is possible that, before a significant crack forms, the non-uniform coefficient is in a range which means the cracking of concrete is always induced by a typical non-uniform corrosion. More researches are necessary, especially experimental results, to clarify the effects of different underlying parameters on k and then formulate an analytical function for k. Figure 7 shows the corrosion rust distribution under the varying k and corrosion degrees. It can be seen that, as corrosion progresses, the distribution of corrosion rust approaches uniform when k decreases.

$T_d(\theta)$ is used as the displacement boundary condition in modelling the cracking of concrete cover. According to Equations (4) and (24), $T_d(\theta)$ can be expressed as follows:

$$T_d(\theta) = (\alpha - 1)\pi R \eta \times \frac{e^{k\cos(\theta-\mu)}}{2\pi I_0(k)} \tag{25}$$

When the corrosion process starts, corrosion rusts first fill in the annular porous layer in concrete around the reinforcing bar, often referred to as "porous zone". This initial stage normally does not produce stresses in concrete. Taking into account the "porous zone" with thickness T_0, the displacement boundary condition $T_d(\theta)$ can be modified as follows:

$$T_d(\theta) = \left\langle (\alpha - 1)\pi R \eta \times \frac{e^{k\cos(\theta-\mu)}}{2\pi I_0(k)} - T_0 \right\rangle \tag{26}$$

where < > is the Macaulay bracket which means the displacement expansion boundary $T_d(\theta)$ will be regarded as zero if the value is less than zero. Figure 8 shows the expansion displacement $T_d(\theta)$ as a function of θ under different values of non-uniform coefficient k. The input parameters are listed in Table 2. The corrosion products accumulate from 150° to 210° for k=25, 120° to 240° for k=5, 90° to 270° for k=2, 60° to 300° for k=1.1 and uniform corrosion for k=0, respectively. Although the total amount of corrosion products for each of the above-mentioned cases is the same, the expansion amount of corrosion products W_m is different because of different amount of corrosion products filling in the "porous zone".

Some researchers have tried to describe the localised or pitting corrosion by a factor of the maximum pitting penetration over the corrosion thickness of general corrosion [10-13]. It has been found that this factor ranges from about 4 to 8 in natural conditions and 5 to 13 in accelerated testing of reinforced concrete. In this model, a factor β is expressed as follows:

$$\beta = \frac{T_{co-st,k}(\pi)}{T_{co-st,k=0}(\pi)} \tag{27}$$

Where $T_{co-st,k}(\pi)$ is the maximum corroded rebar thickness of non-uniform corrosion and $T_{co-st,k=0}(\pi)$ is the corroded rebar thickness of uniform corrosion. According to Equations (2) and (24), $T_{co-st,k}(\pi)$ and $T_{co-st,k=0}(\pi)$ can be derived respectively as follows:

$$T_{co-st,k}(\pi) = \pi R \eta \times \frac{e^k}{2\pi I_0(k)} \tag{28}$$

$$T_{co-st,k=0}(\pi) = \pi R \eta \times \frac{1}{2\pi I_0(0)} \tag{29}$$

By substituting Equations (28) and (29) into Equation (27), β can be expressed as follows:

$$\beta = \frac{e^k}{2\pi I_0(k)} \times 2\pi I_0(0) \tag{30}$$

β can be calculated via Equation (30) and compared with k originally proposed in this study, as shown in Figure 8(a).

5 MESO-SCALE DISCRETE CRACK MODEL FOR FRACTURE OF CONCRETE

In this paper, concrete is modelled as a three-phase (i.e., consisting of mortar, aggregates and ITZ) material. The shape of aggregate is simplified to a random polygon with 3-7 sides. The aggregate size distribution can be represented by a grading curve, which is usually expressed in terms of cumulative percentage passing through a series of sieves with different opening sizes. A typical gradation of aggregate size distribution is listed in Table 3 [33]. For simplicity, only coarse aggregates larger than 2.4 mm are modelled in this study, while fine aggregates and cement are treated as mortar phase. Coarse aggregates generally occupy 40% of the whole volume of concrete. A similar algorithm for generating polygonal aggregate proposed by Pan et al. [34] is devised in this study. There is no overlapping of aggregates in the generation process. The script for producing the 3-phase structure is written in Python which controls the drawings in AutoCAD; the structure is then imported into FE software (i.e., ABAQUS) for analysis.

Figure 9 shows the mesh of the meso-scale RC cover structure with middle and corner rebars. The size of the RC structure is set 150×150 mm and the thickness of concrete cover is 40 mm. Two types of elements are employed in this study, i.e., a 4-node cohesive element for interfaces between the triangle elements and a 3-node plane strain element for the bulk mortar and aggregates. To model arbitrary cracking in concrete, the cohesive elements are embedded at the interfaces throughout the mesh; very fine mesh is produced to ensure random crack paths. The insertion process of cohesive elements is accomplished by an in-house script written in Python. First, all individual nodes are replaced by certain number of new nodes at the same location. The number of newly created nodes depends on the number of the elements connecting to the original node. Second, the newly created nodes at the interface between two triangle elements are identified and linked to form a cohesive element. Figure 10 shows the inserted cohesive elements at the interface of aggregate and mortar, as well as in the aggregates and the mortar. Therefore, the developed model is capable of simulating crack propagation both at the interface and in the bulk mortar and aggregates, depending on their material properties. However, the mechanical properties of aggregates are normally considerably stronger than mortar and the ITZ; thus it is in general very rare to have a crack breaking through an aggregate. In this paper, fracture properties are only assigned in the ITZ and mortar to simulate cracking, in light of reducing computational cost. The numbers of elements for the two models, i.e., cases for corner and middle rebars respectively, are shown in Table 4.

Under the expansive force induced by the accumulation of corrosion products, the concrete cover is predominantly controlled by tension failure and shear failure in case of non-uniform expansion. Therefore, the compressive property of concrete can be assumed elastic without defining the compression failure. Different from some special cases where shearing is not an issue (e.g., [35]), the shearing properties of the material phases affect the cracking paths and structural failure under heterogeneous assumption [36]. Due to the lack of experimental data, the shear strength and Mode-II fracture energy were assumed to be the same as these of Mode-I [25, 37, 38]. The constitutive stress-displacement relation ($\sigma - \delta$) under tension, can be shown in Figure 11. The tensile stress linearly increases until its maximum value, i.e., tensile strength $f_t^{'}$; such a linearity is determined by a penalty stiffness K_p. After reaching the peak value, the tensile stress decreases, following certain strain softening rules, e.g., linear, bi-linear, exponential, etc. The area underneath the curve in Figure 12 is known as the fracture energy G_f. As discussed, aggregate is assumed elastic without defining its damage properties.

The fracture properties of ITZ play an important role in meso scale fracture modelling of concrete [25, 39]. However, it is very hard to obtain the tensile strength and fracture energy of ITZ by experimental tests. Very limited experimental results indicated that the tensile strength of ITZ is about 1/16 to 3/4 of the strength of mortar [39, 40]. Rao and Prasad found the fracture toughness of ITZ varies from 4% to 34% of mortar which is affected by the roughness of aggregates [40]. Tregger et al. found the fracture energy of ITZ is about 0.5 time of that of mortar by experiments [41]. Some researchers simulated the meso scale fracture of concrete under direct tension load and assumed the tensile strength and fracture energy of ITZ both are 0.5 time of those of mortar [25, 37]. Therefore, the tensile strength of

ITZ is regarded as 0.5 time of that of mortar in this paper. Due to the failure of ITZ is more brittle than mortar [42], the fracture energy of ITZ is assumed as 0.25 time of that of mortar. The values for all the basic parameters are shown in Table 5. It should be mentioned the effect of aggregate size and roughness on properties of ITZ is not considered in this paper.

6 SIMULATION RESULTS AND DISCUSSION

Figure 12 shows the crack propagation process induced by corrosion of the middle rebar for non-uniform coefficient *k*=2. Cohesive elements with damage variable *D* equal to 1 (i.e. complete failure) are plotted in red. It can be found that a few micro cracks are first initiated at the aggregate-mortar interfaces near the top surface of the concrete cover. As corrosion continues, the micro cracks are then connected to form a dominant crack propagating from the concrete surface to the rebar. The phenomenon that a crack propagates from concrete surface towards the reinforcement has a good agreement with the experiments [43]. When the corrosion degree increases to 0.15%, new micro cracks are generated at the aggregate-mortar interfaces at the right of the rebar. Finally, three macro cracks are formed, as shown in Figure 12(d). Amongst these three discrete cracks, the top one has the largest opening. Unlike macroscale fracture modelling which considers concrete as a homogeneous material [17], micro cracks always start first at the ITZ before they are connected and form a macro discrete crack. This is because the strength and fracture energy of ITZ cohesive elements are significantly lower than those of mortar. As such, the developed meso-scale fracture model is advantageous compared with most existing concrete fracture models [27, 36] in terms of capturing microcracks in different material phases prior to the occurrence of any dominating visible cracks. It has been found that the effect of aggregate randomness on concrete tensile strength and softening is limited [37, 38]. As the corrosion develops to the stage where the tensile stress reaches the tensile strength, concrete is cracked. The aggregate randomness almost has no effect on the initial cracking. Further, crack deflection will occur when the crack path is around an aggregate or a weaker ITZ. However, the general crack pattern and crack width is quite close to each other under the same aggregate fraction, grading curve and non-uniform corrosion coefficient.

The cracking patterns under different corrosion non-uniform coefficient k are plotted in Figure 13. It should be mentioned that the computational simulations do not converge for k=25 beyond corrosion degree 0.08% and k=5 beyond corrosion degree 0.23%, respectively, due to severe local damage. It can be found that the non-uniform coefficient of corrosion has a significant effect on the cracking patterns of the concrete cover. For k=0, i.e., uniform corrosion, two cracks appear, as shown in Figure 13(a). The top crack is the dominant crack while the other one develops after the top crack. For uniform corrosion, the location of the surface crack may be related to the shape and size of aggregates, cover thickness and diameter of rebar. For non-uniform corrosion of middle rebar, there are three cracks, namely, top crack, left crack and right crack. It has been found that the larger the non-uniform coefficient is, the left and right cracks are closer to the top surface of concrete cover. When the non-uniform coefficients are 5 and 25, the left and right cracks are located near the horizontal line which causes delamination failure of the cover. This phenomenon has a good agreement with the crack patterns found in Malumbela's experiments [44].

Crack width is an important parameter with regards to the durability of concrete structures. Upon measuring the distances between the nodes of specific cohesive elements of the surface cracks, the crack width evolution of the surface cracks as a function of corrosion degree for different non-uniform coefficients are shown in Figure 14. It can be seen that the surface crack suddenly increases to about 0.03 mm; after that, the surface crack width grows up almost linearly. A very small corrosion degree (less than 0.25%) can cause concrete cover cracking. Moreover, it has been found that the larger the non-uniform coefficient is, the smaller the corrosion degree at surface cracking is. Although the final crack width for k=25 and k=0 is small, it can be predicted that more uniform corrosion can lead to smaller crack width under given corrosion degree. Most previous studies [1, 3, 6, 7, 45] assumed uniform corrosion which overestimated the volume that is occupied by corrosion products and therefore underestimated the time to surface cracking and crack width development.

Figure 15 illustrates the crack propagation process induced by corrosion of the corner rebar for non-uniform coefficient k=2. As discussed, micro cracks are first initiated at the aggregate-mortar interfaces at the right of the rebar before a dominant crack forms. The other crack appears at the upper left corner of rebar and continues to propagate to the surface of concrete.

The cracking patterns induced by corrosion of corner rebar under different corrosion non-uniform coefficient k are plotted in Figure 16. The computation did not converge for k=25 beyond the corrosion degree 0.10%. For uniform corrosion, there are two macro cracks at right side of the rebar and one macro crack at top of the rebar. The cracking pattern for uniform corrosion is related to the size and shape of aggregates and the cracks will cause a spalling failure of the concrete cover. For non-uniform corrosion, larger non-uniform coefficient can cause the incline of the macro cracks towards the maximum thickness of the corrosion layer (i.e., $\theta=\pi$) and the angle of the spalling failure becomes smaller. Further, for a relatively large non-uniform coefficient, some micro cracks appear around the maximum thickness of corrosion layer, which conforms to the experimental results in Zhao et al. [20].

Figure 17 shows the surface crack width as a function of corrosion degree under different non-uniform coefficients for the corner rebar case. When the non-uniform coefficient increases from 0 to 25, the corrosion degree to cause surface cracking is decreased from about 0.21% to 0.05%. It has been found that larger non-uniform coefficient can lead to greater slope of curve of surface crack width as a function of corrosion degree. This means that, given the same corrosion degree, the crack width for more localised corrosion is larger than that for uniform corrosion.

It has been reported that the thickness of the "porous zone" between reinforcement and concrete considerably affect the cracking of concrete cover [16]. Figure 18 illustrates the effect of thickness of the "porous zone" on the cracking pattern. It can be seen that as the thickness of the "porous zone" (T_0) increases, the crack widths for all three discrete cracks reduce. Moreover, the two side cracks tend to incline towards the top surface, when T_0 increases. Figure 19 shows the effect of T_0 on surface crack width for corrosion non-uniform coefficient k=0 and 2. It can be seen that, for a large thickness of "porous zone", more corrosion products are required to fracture the concrete cover. When T_0 increases by 12.5 µm, the corrosion degree to surface cracking increases by about 0.05% for k=2 and 0.10% for k=0. Therefore, the effect of thickness of the "porous zone" on surface crack width varies from corrosion non-uniform coefficient. The smaller the corrosion non-uniform coefficient is, the thickness of the "porous zone" affects the corrosion degree to surface cracking more significantly. It should be mentioned that, the value of T_0 is a virtual concept for calculating the corrosion-accommodating region, which is related to water/cement ratio and corrosion rate [46]. For non-uniform corrosion with different non-uniform coefficients, the corrosion products required for filling in the "porous zone" are different.

7 CONCLUSIONS

In this paper, a von Mises corrosion model was derived to formulate the corrosion expansion around the reinforcing bar. The model was simply composed of three parameters including the corrosion degree indicator λ, the non-uniform coefficient k and the location of the maximum thickness of the corrosion layer μ. The results predicted by the developed model have been compared with experimental results and a good agreement has been achieved. Compared with the existing models, the von Mises model has the best accuracy in fitting with the experimental data and fewer parameters with direct physical meanings. Moreover, the thickness of the "porous zone" between reinforcement and concrete has also been taken into account. Two meso-scale models consisting of aggregates, mortar and ITZ were built for the cases of the middle and corner rebars, respectively. The concrete cover cracking induced by corrosion of the middle and corner bars with five different non-uniform coefficients were simulated. Moreover, the crack width developments as a function of corrosion degree were obtained. It has been found that the larger the non-uniform coefficient is, the smaller the corrosion degree at surface cracking is. It has also been found that the thickness of the "porous zone" can dramatically change the amount of rust that is required to fracture the concrete cover; meanwhile, the smaller the non-uniform coefficient is, the more the thickness of the "porous zone" affects the corrosion degree to the surface cracking.

ACKNOWLEDGEMENTS

Financial support from European Commission via the Marie Sklodowska-Curie H2020 RISE scheme under 645696 and National Key R&D Plan of China (Grant No: 2016YFC0600803) is gratefully acknowledged. The first author would also like to thank China Scholarship Council for supporting his PhD research at the University of Strathclyde, UK.

REFERENCES

[1] C.Q. Li, S.T. Yang, Prediction of concrete crack width under combined reinforcement corrosion and applied load, Journal of Engineering Mechanics-ASCE, 137 (2011) 722-731.

[2] C. Andrade, F.J. Molina, C. Alonso, Cover cracking as a function of rebar corrosion: Part 1-experiment test, Materials and Structures, 26 (1993) 453-454.

[3] Y. Liu, R.E. Weyers, Modelling the time-to-corrosion cracking in chloride contaminated reinforced concrete structures, ACI Materials Journal, 95 (1998) 675-681.

[4] S.J. Pantazopoulou, K.D. Papoulia, Modeling cover cracking due to reinforcement corrosion in RC structures, Journal of Engineering Mechanics-ASCE, 127 (2001) 342-351.

[5] K. Bhargava, A.K. Ghosh, Y. Mori, S. Ramanujam, Model for cover cracking due to rebar corrosion in RC structures, Engineering Structures, 28 (2006) 1093-1109.

[6] K. Bhargava, A.K. Ghosh, Y. Mori, S. Ramanujam, Modeling of time to corrosion-induced cover cracking in reinforced concrete structures, Cement and Concrete Research, 35 (2005) 2203-2218.

[7] C. Lu, W. Jin, R. Liu, Reinforcement corrosion-induced cover cracking and its time prediction for reinforced concrete structures, Corrosion Science, 53 (2011) 1337-1347.

[8] C.Q. Li, R.E. Melchers, J.J. Zheng, Analytical model for corrosion-induced crack width in reinforced concrete structures, ACI Structural Journal, 103 (2006) 479-487.

[9] C. Cao, M.M.S. Cheung, B.Y.B. Chan, Modelling of interaction between corrosion-induced concrete cover crack and steel corrosion rate, Corrosion Science, 69 (2013) 97-109.

[10] J.A. González, C. Andrade, C. Alonso, S. Feliu, Comparison of rates of general corrosion and maximum pitting penetration on concrete embedded steel reinforcement, Cement and Concrete Research, 25 (1995) 257-264.

[11] B.S. Jang, B.H. Oh, Effects of non-uniform corrosion on the cracking and service life of reinforced concrete structures, Cement and Concrete Research, 40 (2010) 1441-1450.

[12] A. Chen, Z. Pan, R. Ma, Mesoscopic simulation of steel rebar corrosion process in concrete and its damage to concrete cover, Structure and Infrastructure Engineering, 13 (2016) 478-493.

[13] B. Šavija, M. Luković, J. Pacheco, E. Schlangen, Cracking of the concrete cover due to reinforcement corrosion: A two-dimensional lattice model study, Construction and Building Materials, 44 (2013) 626-638.

[14] T. Pan, Y. Lu, Stochastic Modeling of Reinforced Concrete Cracking due to Nonuniform Corrosion: FEM-Based Cross-Scale Analysis, Journal of Materials in Civil Engineering, 24 (2012) 698-706.

[15] Y. Yuan, Y. Ji, Modeling corroded section configuration of steel bar in concrete structure, Construction and Building Materials, 23 (2009) 2461-2466.

[16] S.T. Yang, K.F. Li, C.Q. Li, Analytical model for non-uniform corrosion-induced concrete cracking, Magazine of Concrete Research, 90 (2018) 1-10.

[17] X. Xi, S. Yang, Time to surface cracking and crack width of reinforced concrete structures under corrosion of multiple rebars Construction and Building Materials, 155 (2017) 114-125.

[18] Y. Zhao, A.R. Karimi, H.S. Wong, B. Hu, N.R. Buenfeld, W. Jin, Comparison of uniform and non-uniform corrosion induced damage in reinforced concrete based on a Gaussian description of the corrosion layer, Corrosion Science, 53 (2011) 2803-2814.

[19] Y. Zhao, B. Hu, J. Yu, W. Jin, Non-uniform distribution of rust layer around steel bar in concrete, Corrosion Science, 53 (2011) 4300-4308.
[20] Y. Zhao, J. Yu, B. Hu, W. Jin, Crack shape and rust distribution in corrosion-induced cracking concrete, Corrosion Science, 55 (2012) 385-393.
[21] Y. Zhao, X. Zhang, H. Ding, W. Jin, Non-uniform distribution of a corrosion layer at a steel/concrete interface described by a Gaussian model, Corrosion Science, 112 (2016) 1-12.
[22] K.K. Tran, H. Nakamura, K. Kawamura, M. Kunieda, Analysis of crack propagation due to rebar corrosion using RBSM, Cement and Concrete Composites, 33 (2011) 906-917.
[23] D. Qiao, H. Nakamura, Y. Yamamoto, T. Miura, Crack patterns of concrete with a single rebar subjected to non-uniform and localized corrosion, Construction and Building Materials, 116 (2016) 366-377.
[24] J. Zhang, X. Ling, Z. Guan, Finite element modeling of concrete cover crack propagation due to non-uniform corrosion of reinforcement, Construction and Building Materials, 132 (2017) 487-499.
[25] W. Ren, Z. Yang, R. Sharma, C. Zhang, P.J. Withers, Two-dimensional X-ray CT image based meso-scale fracture modelling of concrete, Engineering Fracture Mechanics, 133 (2015) 24-39.
[26] X. Du, L. Jin, R. Zhang, Modeling the cracking of cover concrete due to non-uniform corrosion of reinforcement, Corrosion Science, 89 (2014) 189-202.
[27] E. Chen, C.K.Y. Leung, Finite element modeling of concrete cover cracking due to non-uniform steel corrosion, Engineering Fracture Mechanics, 134 (2015) 61-78.
[28] L. Jin, R. Zhang, X. Du, Y. Li, Investigation on the cracking behavior of concrete cover induced by corner located rebar corrosion, Engineering Failure Analysis, 52 (2015) 129-143.
[29] X. Ning, R. Qingwen, P. Joe, Y.L. Robert, P. Anil, Nonuniform Corrosion-Induced Stresses in Steel-Reinforced Concrete, Journal of Engineering Mechanics, ASCE, 138 (2012) 338-346.
[30] C. Forbes, M. Evans, N. Hastings, B. Peacock, Statistical Distributions, Fourth ed., John Wiley & Sons, Inc.2010.
[31] D.J. Best, N.I. Fisher, Efficient Simulation of the von Mises Distribution, Journal of the Royal Statistical Society. Series C (Applied Statistics), 28 (1979) 152-157.
[32] C. E, Computational modeling of concrete cracking due to non-uniform steel corrosion in reinforced concrete structures, The Hong Kong University of Science and Technology, 2015.
[33] A.M. Neville, Properties of concrete, Fourth ed., Pearson Education Limited, London, 2006.
[34] Z. Pan, X. Ruan, A. Chen, A 2-D numerical research on spatial variability of concrete carbonation depth at meso-scale, Computers and Concrete, 15 (2015) 231-257.
[35] J.C. Gálvez, D.A. Cendón, J. Planas, Influence of shear parameters on mixed–mode fracture of concrete, International Journal of Fracture, 118 (2002) 163-189.
[36] Z. Yang, X. Frank Xu, A heterogeneous cohesive model for quasi-brittle materials considering spatially varying random fracture properties, Computer Methods in Applied Mechanics and Engineering, 197 (2008) 4027-4039.
[37] Z.J. Yang, X.T. Su, J.F. Chen, G.H. Liu, Monte Carlo simulation of complex cohesive fracture in random heterogeneous quasi-brittle materials, International Journal of Solids and Structures, 46 (2009) 3222-3234.
[38] X.F. Wang, Z.J. Yang, J.R. Yates, A.P. Jivkov, C. Zhang, Monte Carlo simulations of mesoscale fracture modelling of concrete with random aggregates and pores, Construction and Building Materials, 75 (2015) 35-45.

[39] J. Xiao, W. Li, D.J. Corr, S.P. Shah, Effects of interfacial transition zones on the stress–strain behavior of modeled recycled aggregate concrete, Cement and Concrete Research, 52 (2013) 82-99.
[40] G.A. Rao, B.K. Raghu Prasad, Influence of type of aggregate and surface roughness on the interface fracture properties, Materials and Structures, 37 (2004) 328-334.
[41] N. Tregger, D. Corr, L. Graham-Brady, S. Shah, Modeling the effect of mesoscale randomness on concrete fracture, Probabilistic Engineering Mechanics, 21 (2006) 217-225.
[42] D. Corr, M. Accardi, L. Graham-Brady, S. Shah, Digital image correlation analysis of interfacial debonding properties and fracture behavior in concrete, Engineering Fracture Mechanics, 74 (2007) 109-121.
[43] S. Caré, Q.T. Nguyen, K. Beddiar, Y. Berthaud, Times to cracking in reinforced mortar beams subjected to accelerated corrosion tests, Materials and Structures, 43 (2009) 107-124.
[44] G. Malumbela, P. Moyo, M. Alexander, Influence of corrosion crack patterns on the rate of crack widening of RC beams, Construction and Building Materials, 25 (2011) 2540-2553.
[45] C.Q. Li, Time Dependent Reliability Analysis of the Serviceability of Corrosion Affected Concrete Structures, International Journal of Materials and Structural Reliability, 3 (2005) 105-116.
[46] A. Jamali, U. Angst, B. Adey, B. Elsener, Modeling of corrosion-induced concrete cover cracking: A critical analysis, Construction and Building Materials, 42 (2013) 225-237.

LIST OF TABLES

Table 1 Values of basic parameters formulated in the developed von Mises corrosion model

Test data	λ	*k*	*μ*	R^2	**Test data**	λ	*k*	*μ*	R^2
1	0.321	3.122	3.181	0.991	5	0.613	3.362	3.348	0.817
2	0.941	0.555	3.188	0.934	6	0.353	3.232	3.182	0.906
3	0.198	1.832	3.325	0.931	7	0.799	0.923	2.963	0.953
4	0.349	3.285	3.173	0.901	8	1.550	0.689	3.540	0.768

Table 2 Values of basic variables in the example

Symbol	**Values**	**Sources**
R	8 mm	Zhao [19]
T_0	12.5 μm	Liu and Weyers [3]
α	3.83	Liu and Weyers [3, 4]
η	0.26%	Zhao [19]

Table 3 Three-segment gradation of aggregate size distribution [33]

Aggregate size (mm)	Fraction (%)
2.40-4.76	20.2 %
4.76-9.52	39.9%
9.52-19.05	39.9%

Table 4 Number of elements in the computational models

Model	Solid elements for mortar	Solid elements for aggregate	Cohesive elements for mortar	Cohesive elements for aggregate	Interfacial cohesive elements	Total
Middle rebar	12198	8174	15808	9996	4530	50706
Corner rebar	12422	8272	10058	16089	4700	51541

Table 5 Values for geometric and mechanical parameters for different phases

Description	**Symbol**	**Values**
Cover thickness	C	40 mm
Diameter of steel bars	D	16 mm
Young's modulus of aggregate	E_{Agg}	70 GPa [25]
Young's modulus of mortar	E_{Mor}	25 GPa [25]
Poisson's ratio of aggregate	ν_{Agg}	0.2 [25]
Poisson's ratio of mortar	ν_{Mor}	0.2 [25]
Tensile strength of mortar	$f'_{t,Mor}$	6 MPa [25]
Tensile strength of ITZ	$f'_{t,Int}$	3 MPa [25, 39, 40]
Fracture energy of mortar	$G_{f,Mor}$	60 N/m [25]
Fracture energy of ITZ	$G_{f,Int}$	15 N/m [25, 39, 40]

LIST OF FIGURES

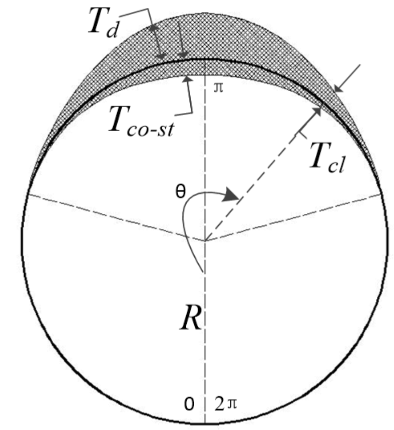

（a）Non-uniform corrosion model

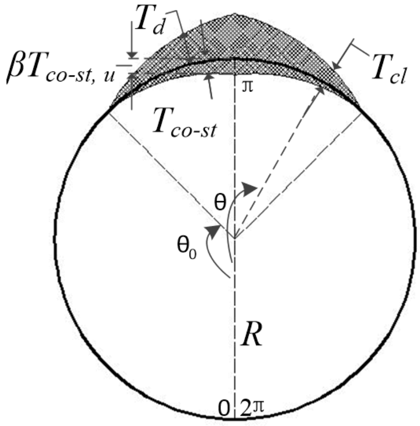

(b) Linear decrease model [11-13]

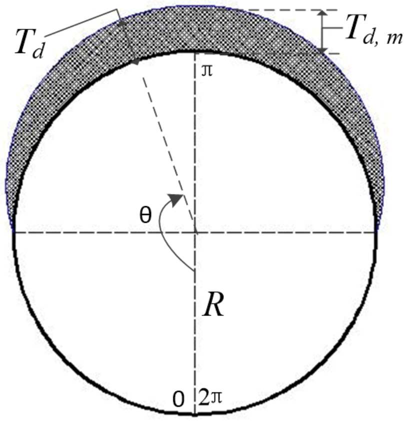

(c) Quadratic semicircle model [14]

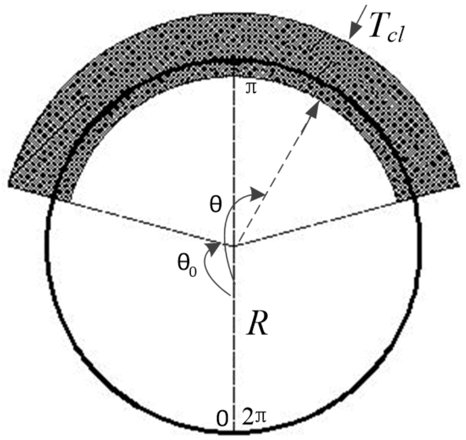

(d) Partly uniform model [22, 23]

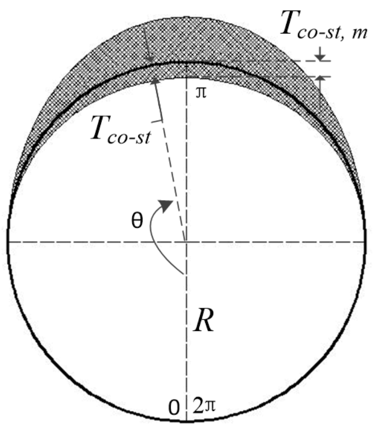

(e) Elliptical model [15]

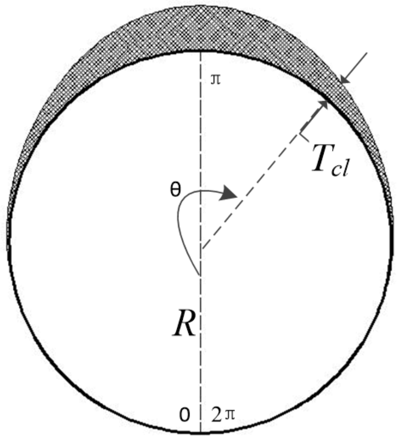

(f) Gaussian model [21]

Figure 1 Various models on corrosion rust progression around the reinforcement in concrete

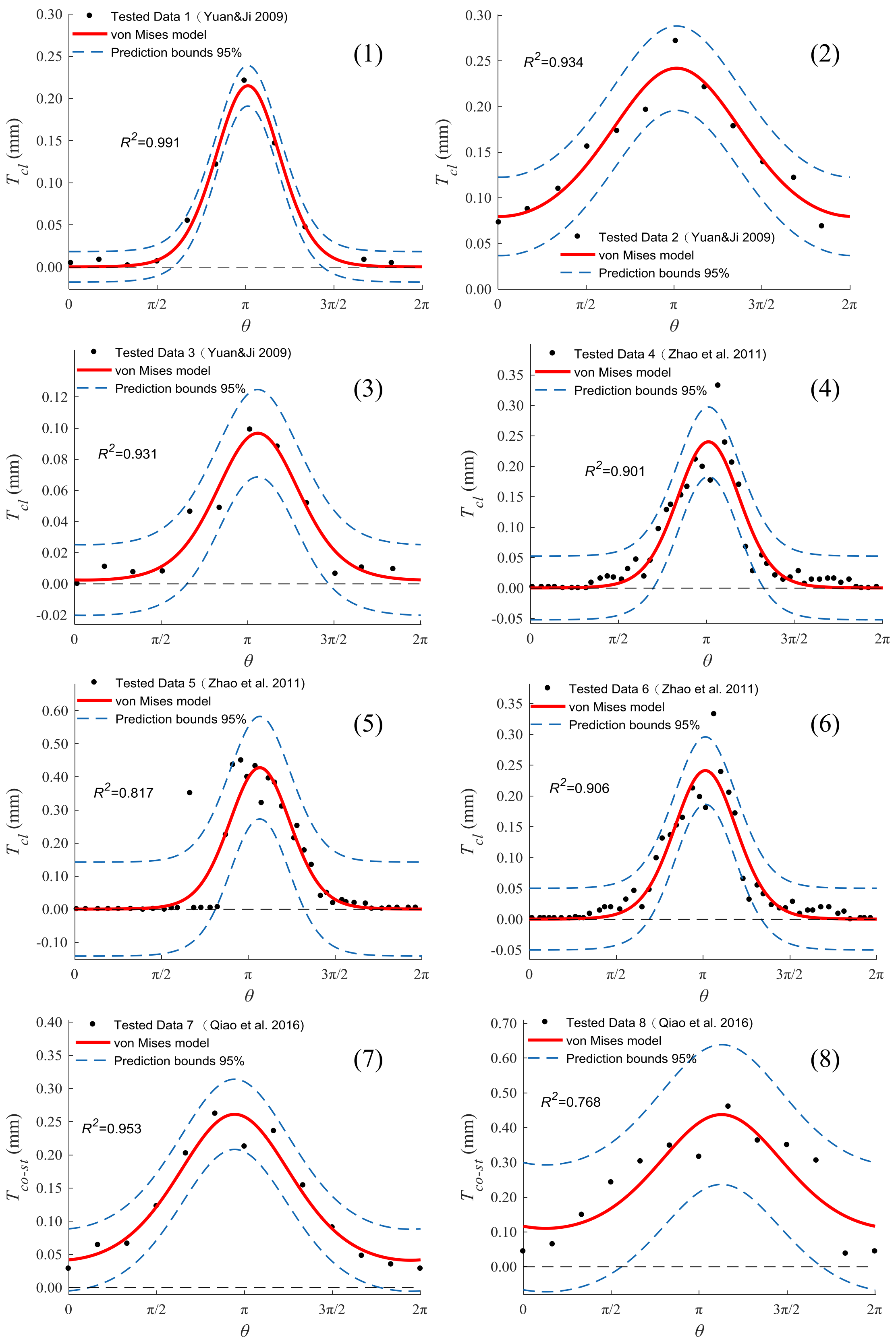

Figure 2 Regression analysis of the developed von Mises model with test data

(Note: the test data 4 and 6 were obtained from corrosion of corner rebar and the others were from corrosion of middle rebar [15, 19, 23])

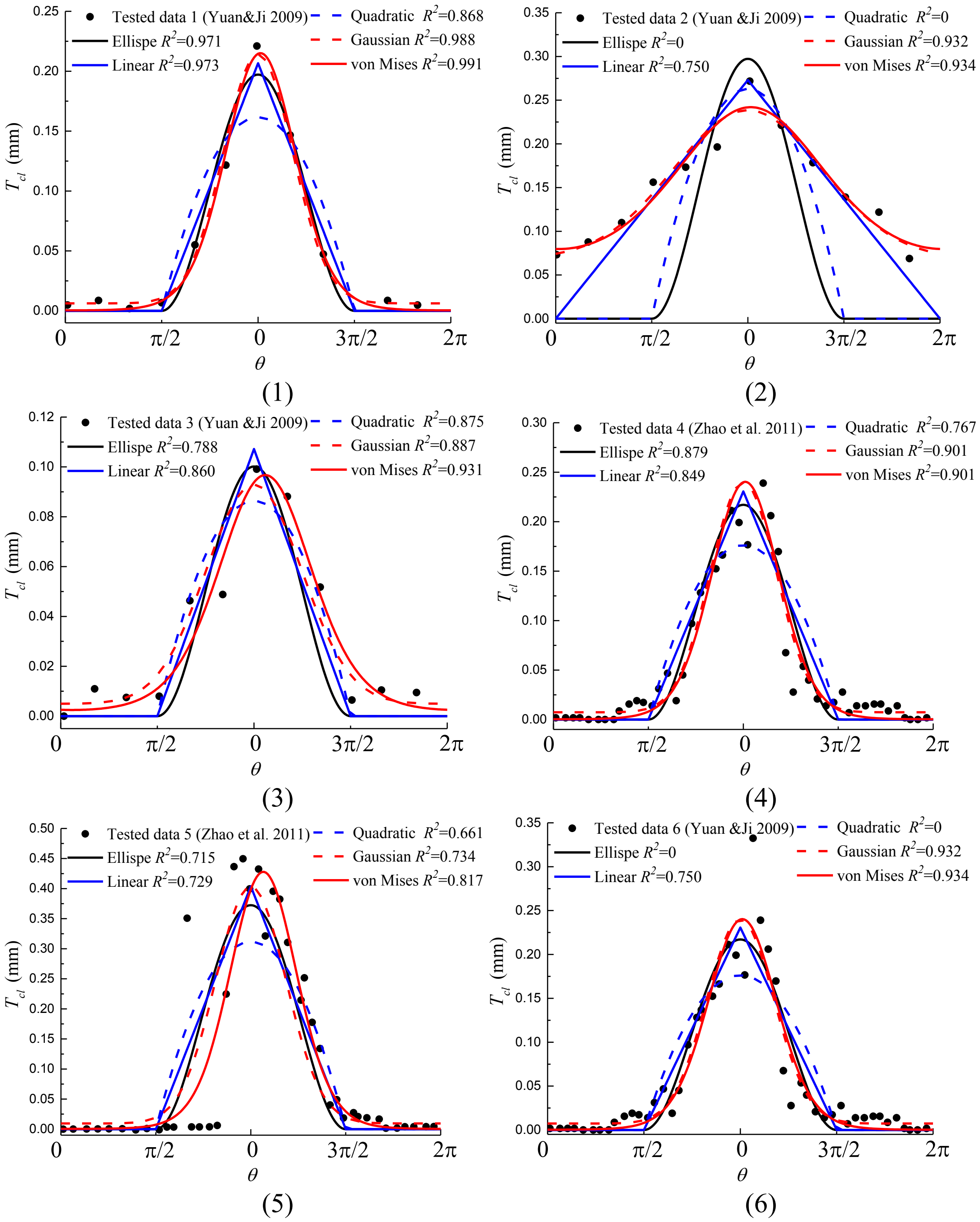

Figure 3 Regression analysis of the existing models with test data

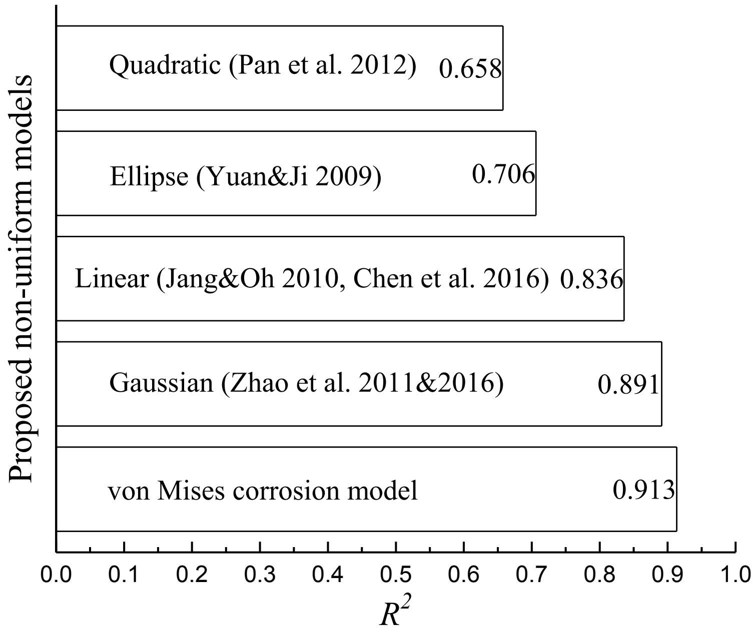

Figure 4 Comparison of average value of R^2 for various corrosion models

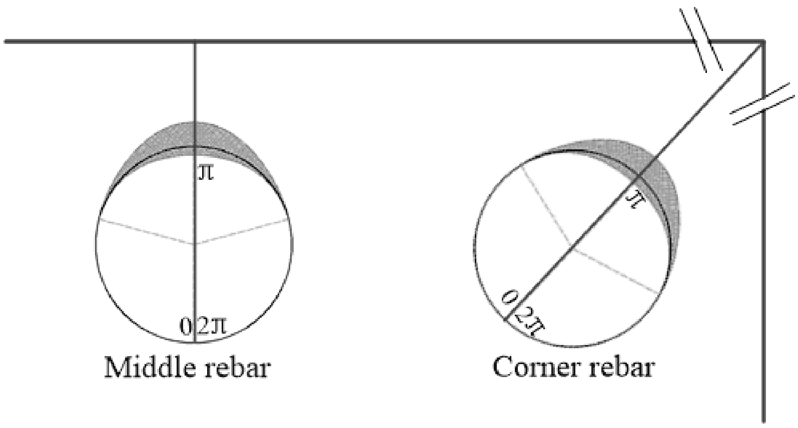

Figure 5 Polar coordinate system defined in experiments [15, 19, 23] and the developed model

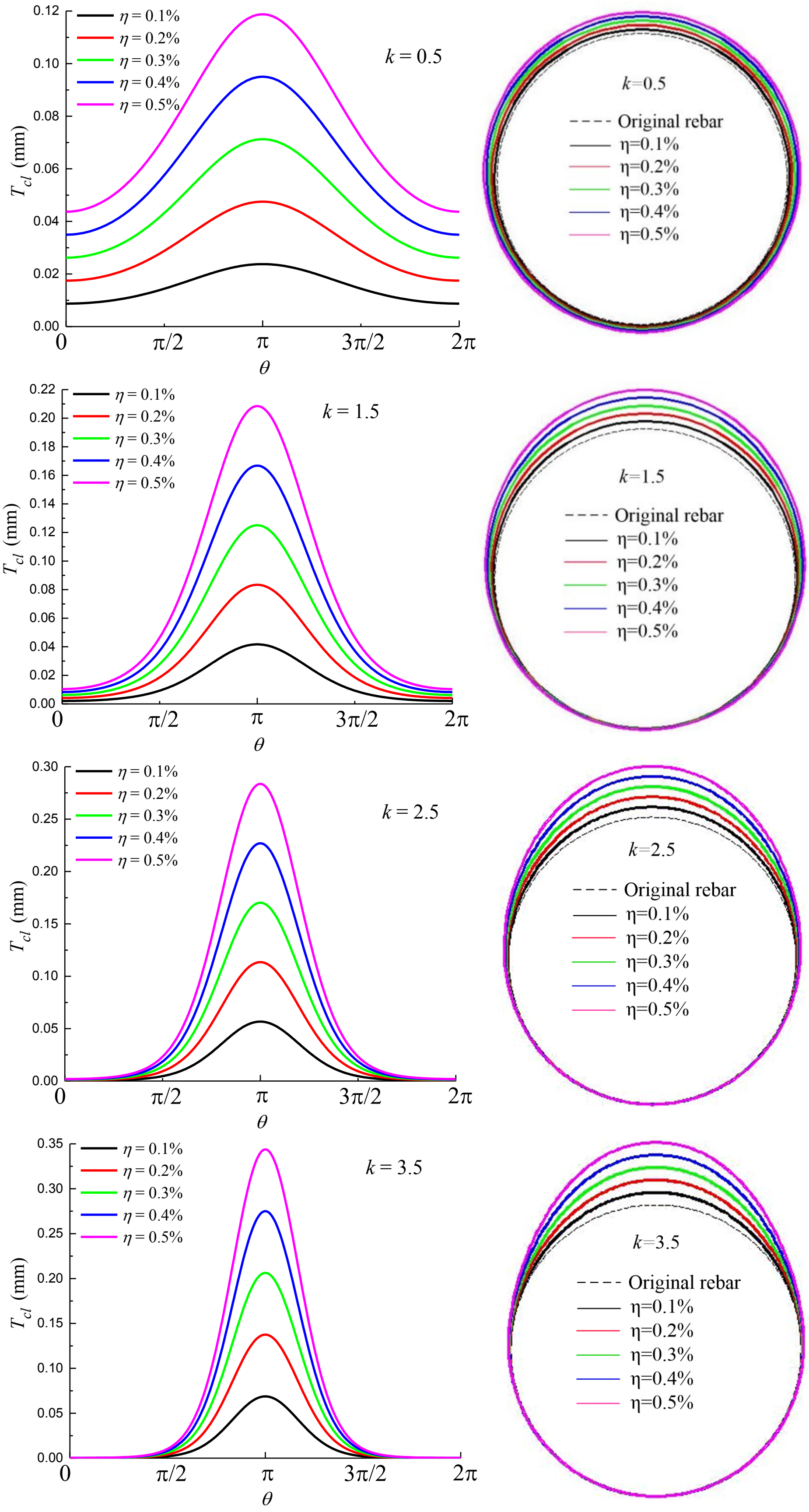

Figure 6 Corrosion rust distributions based on the von Mises model under different values of k and corrosion degree (Note: the deformation scale for the right pictures is 10)

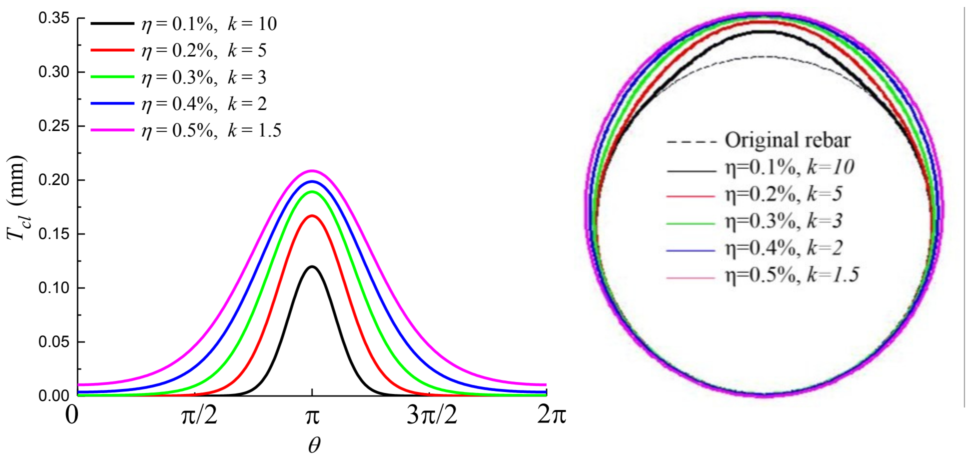

Figure 7 Corrosion rust distributions based on the von Mises model under varying *k* and corrosion degree (Note: the deformation scale for the right picture is 10)

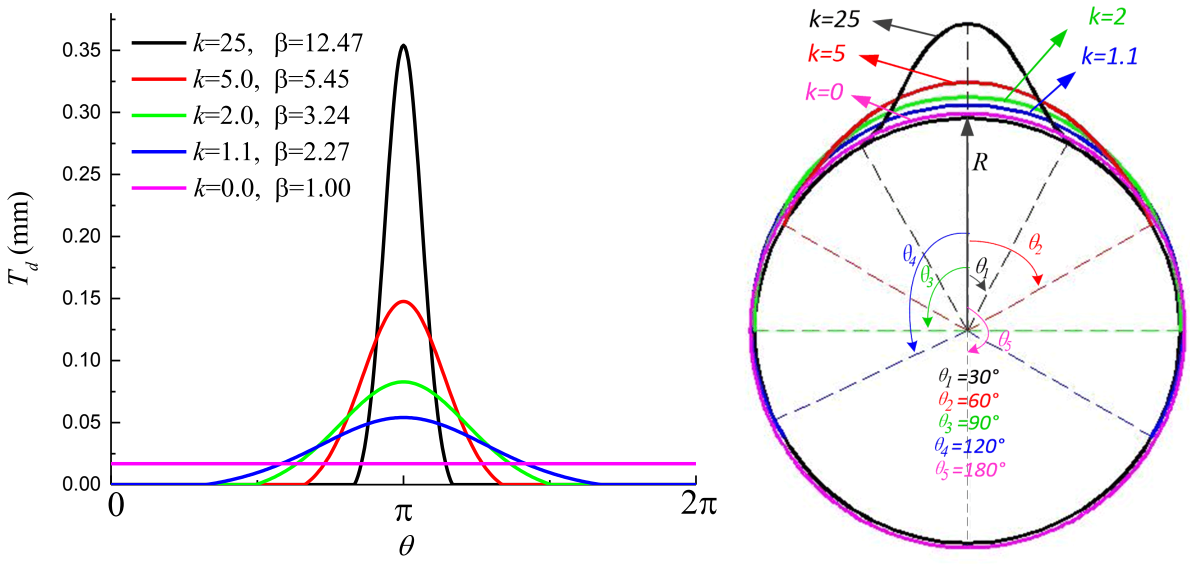

(a) (b) (Scale factor for T_d is10)

Figure 8 Expansion displacement T_d distributions under five different non-uniform coefficients

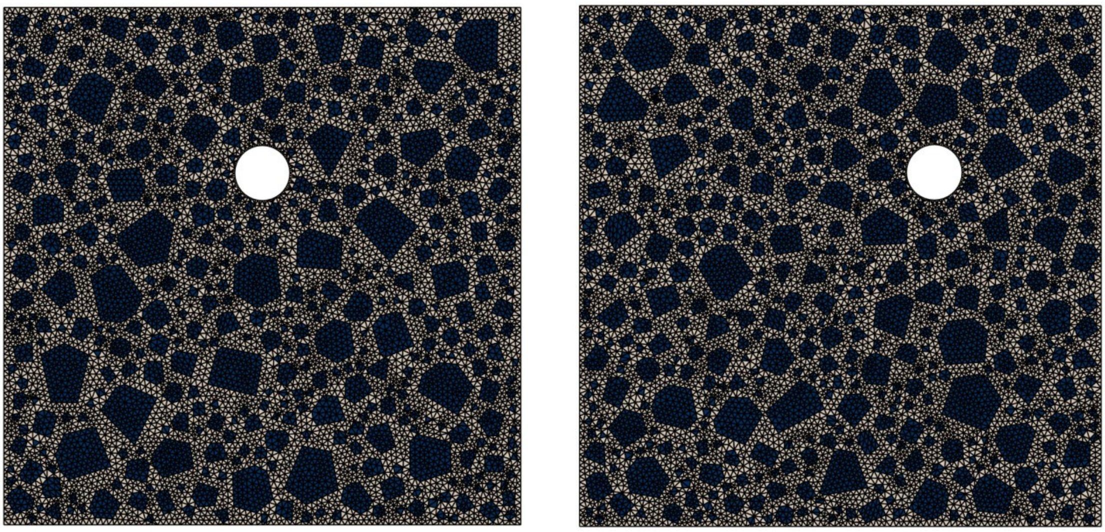

(a) Middle rebar (b) Corner rebar

Figure 9 Meshes for concrete cover structures with middle rebar and corner rebar respectively

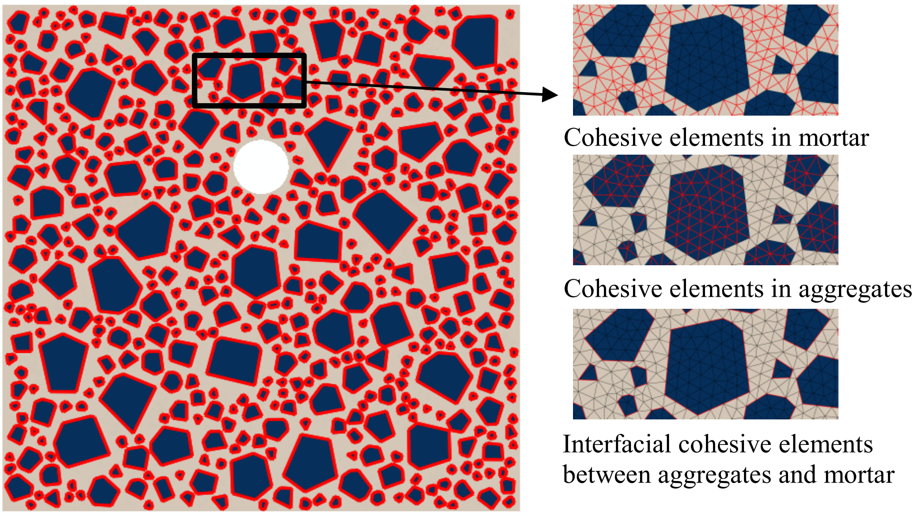

Figure 10 Inserted cohesive elements in the FE mesh

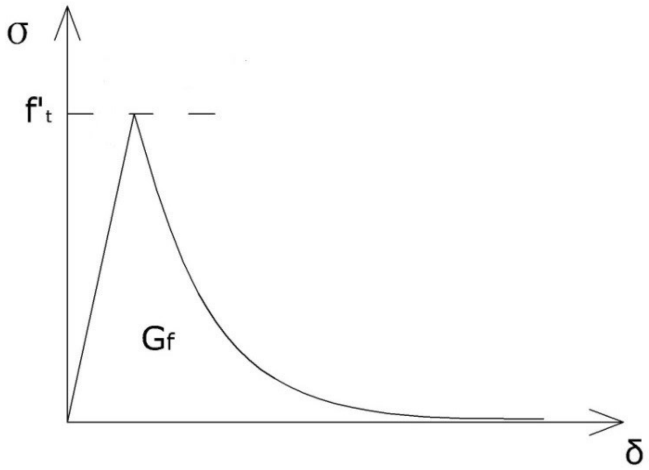

Figure 11 Constitutive relationship of concrete in tension

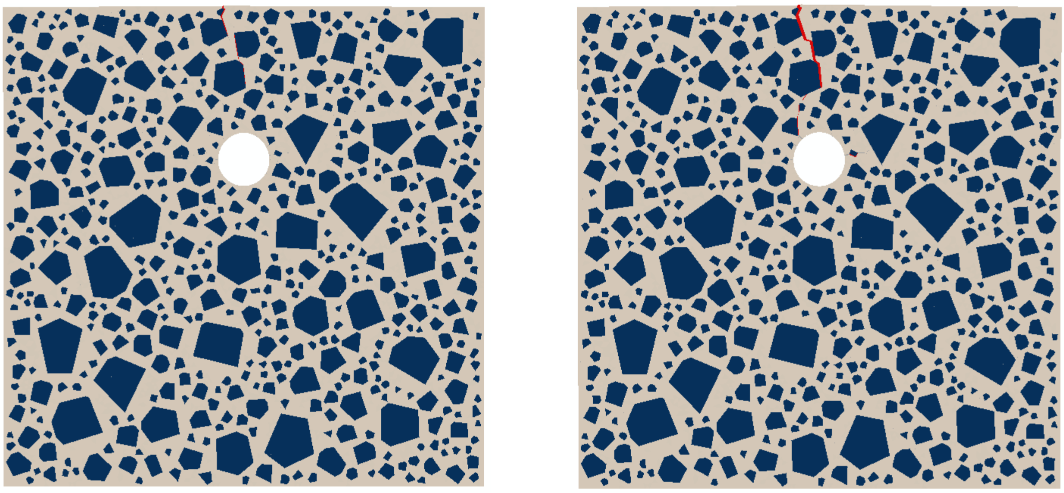

(a) corrosion degree $\eta = 0.11\%$ (b) corrosion degree $\eta = 0.12\%$

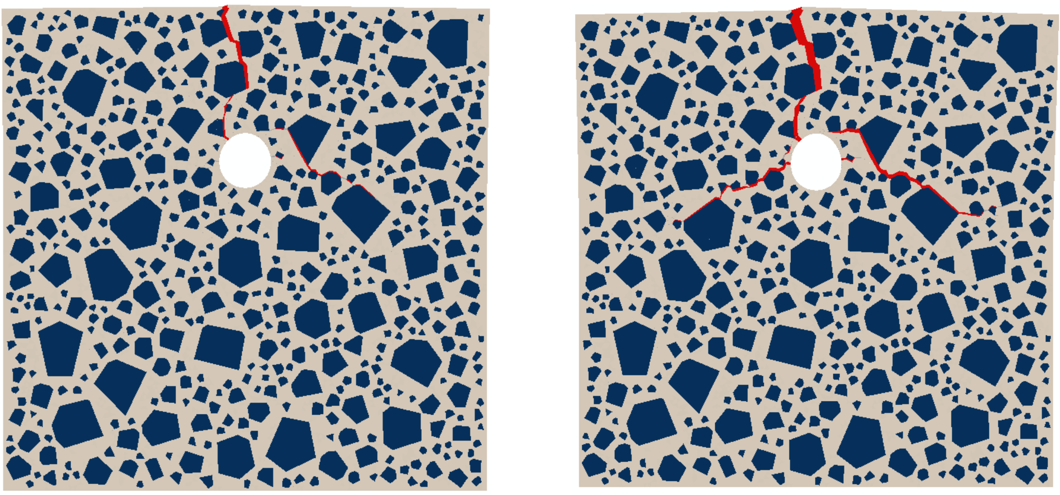

(c) corrosion degree $\eta = 0.15\%$ (d) corrosion degree $\eta = 0.26\%$

Figure 12 Crack propagation induced by corrosion of middle rebar for non-uniform coefficient k=2 (Note: the red regions represent completely cracked cohesive elements, i.e., D = 1.0; Deformation scale: 25)

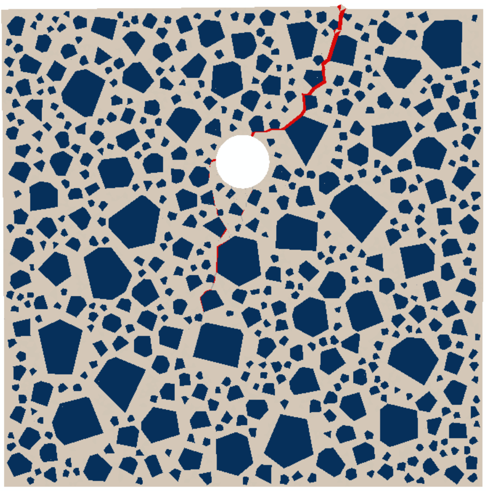

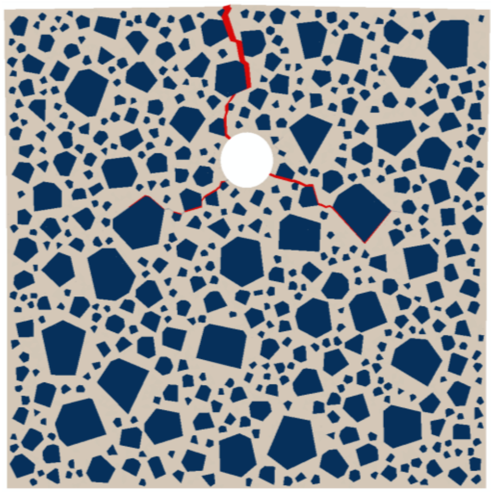

(a) $k = 0, \eta = 0.26\%$ (b) $k = 1.1, \eta = 0.26\%$

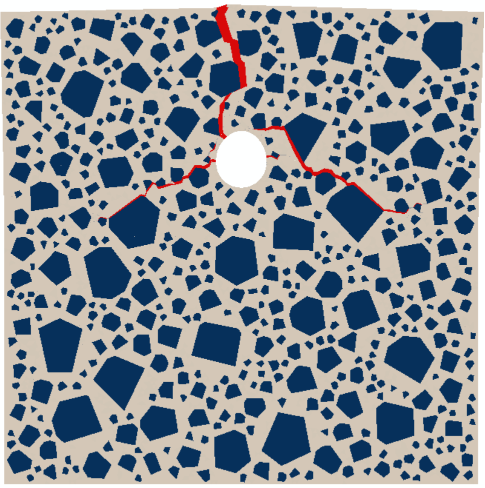

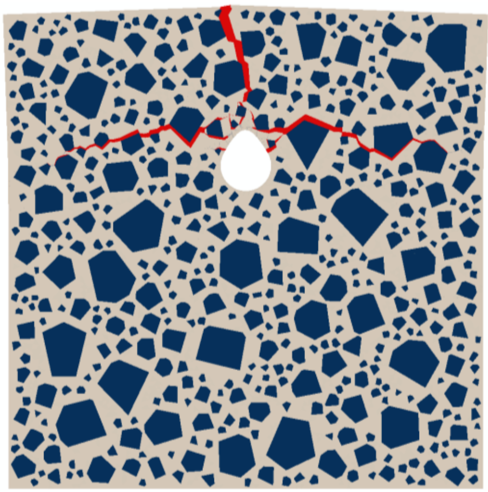

(c) $k = 2, \eta = 0.26\%$ (d) $k = 5, \eta = 0.23\%$

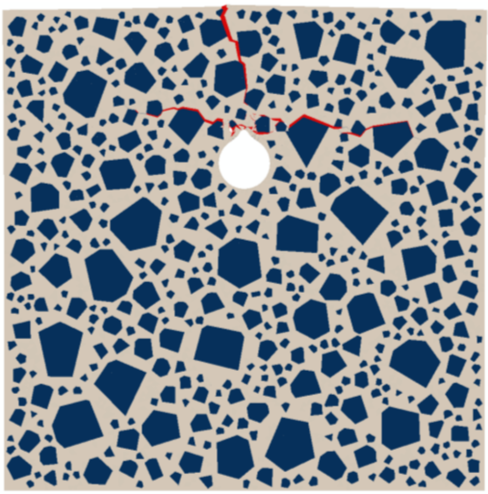

(e) $k = 25, \eta = 0.08\%$

Figure 13 Crack patterns under different corrosion non-uniform coefficient k

(Note: the red regions represent completely cracked cohesive elements, i.e., D = 1.0; Deformation scale: 25)

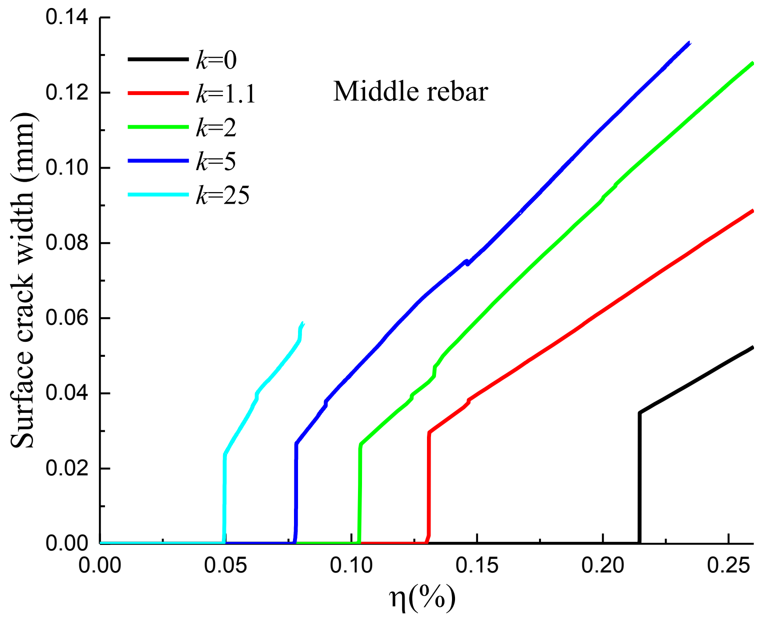

Figure 14 Surface crack width induced by corrosion of middle rebar as a function of corrosion degree η under different non-uniform corrosion coefficient k

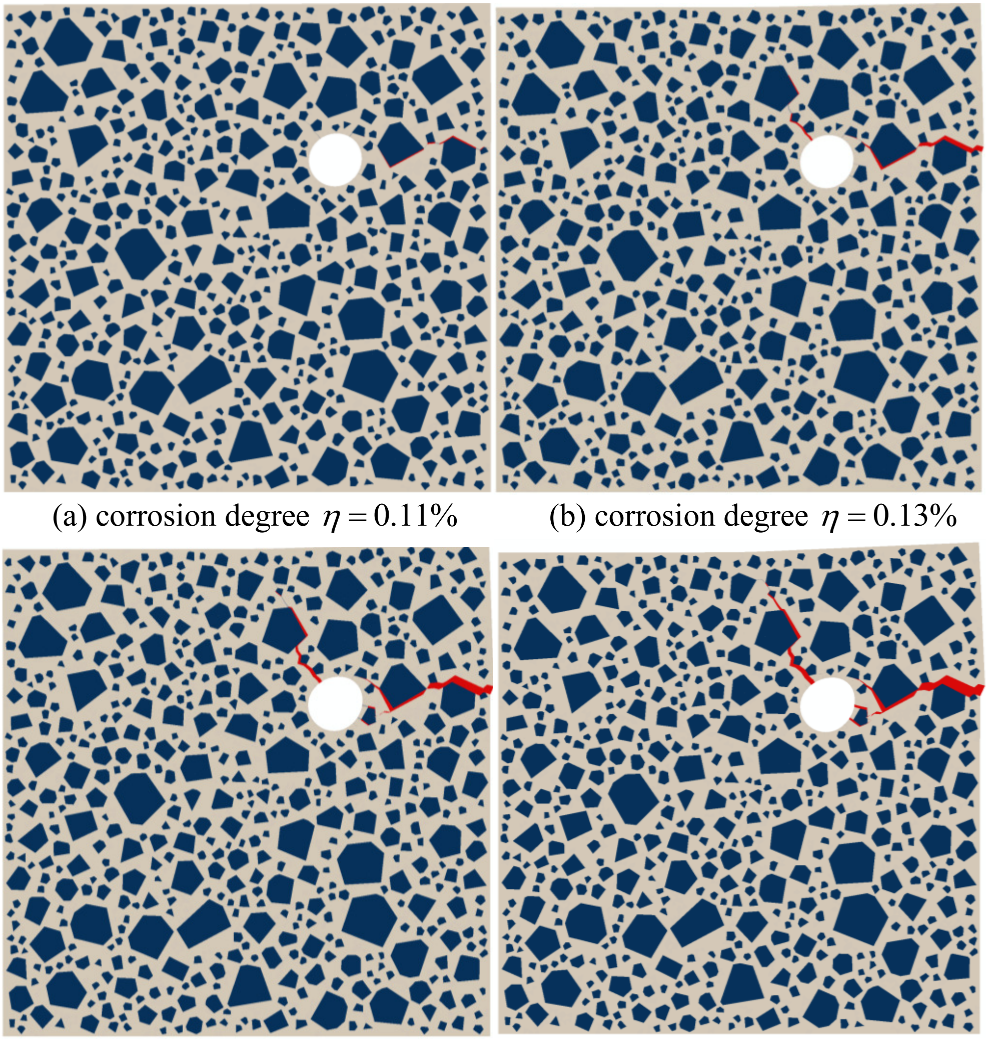

(a) corrosion degree $\eta = 0.11\%$ (b) corrosion degree $\eta = 0.13\%$

(c) corrosion degree $\eta = 0.20\%$ (d) corrosion degree $\eta = 0.26\%$

Figure 15 Crack propagation induced by corrosion of corner rebar for non-uniform coefficient k=2 (Note: the red regions represent completely cracked cohesive elements, i.e., D = 1.0; Deformation scale: 25)

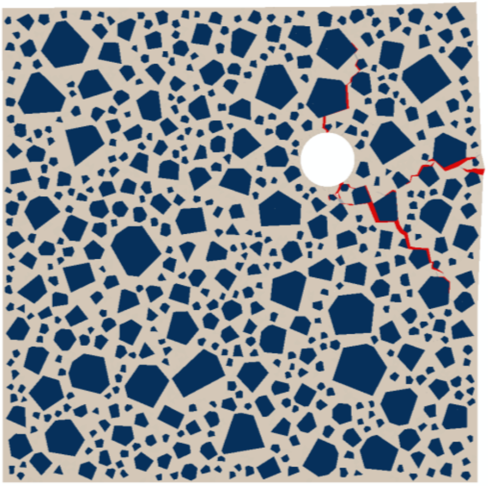

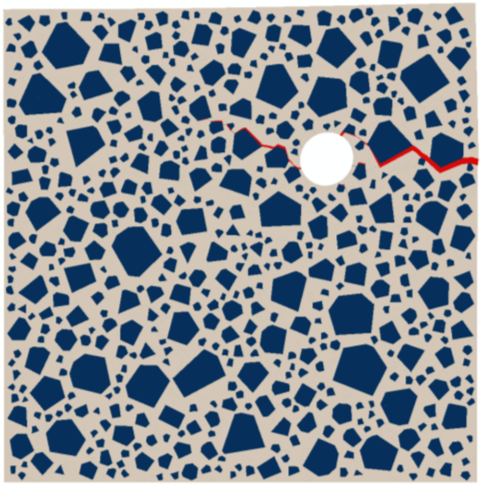

(a) $k=0, \eta=0.26\%$ (b) $k=1.1, \eta=0.26\%$

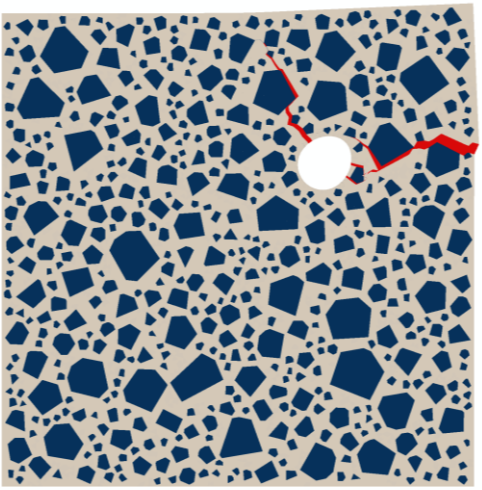

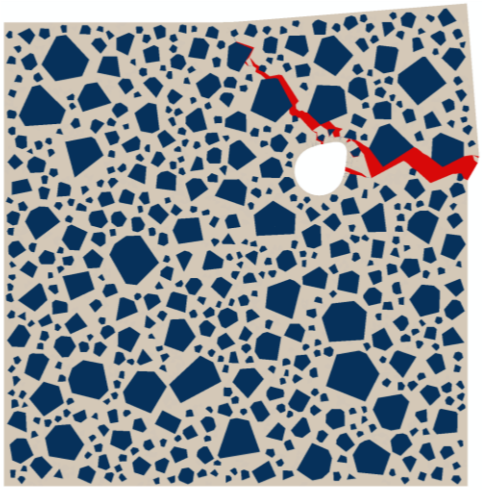

(c) $k=2, \eta=0.26\%$ (d) $k=5, \eta=0.26\%$

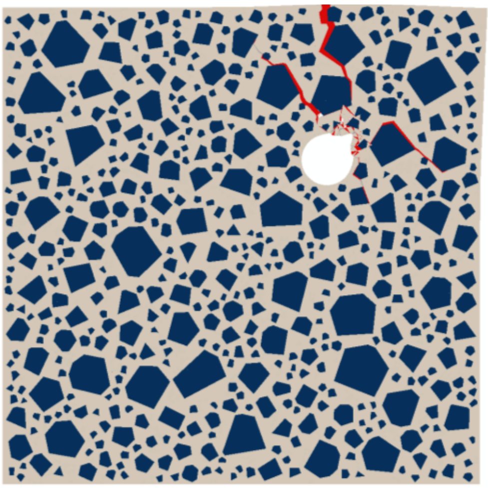

(e) $k=25, \eta=0.10\%$

Figure 16 Crack patterns under different non-uniform corrosion coefficient k
(Note: the red regions represent completely cracked cohesive elements, i.e., $D = 1.0$;
Deformation scale: 25)

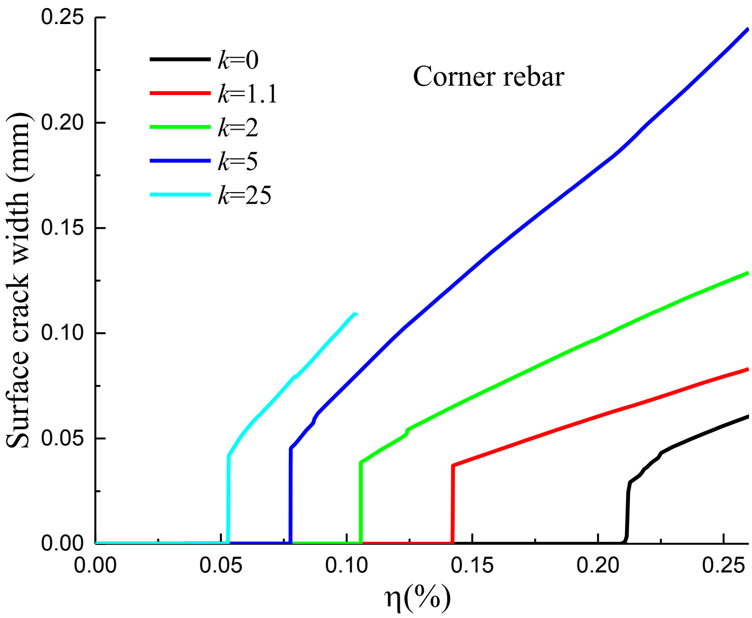

Figure 17 Surface crack width induced by corrosion of corner rebar as a function of corrosion degree η under different non-uniform coefficient k

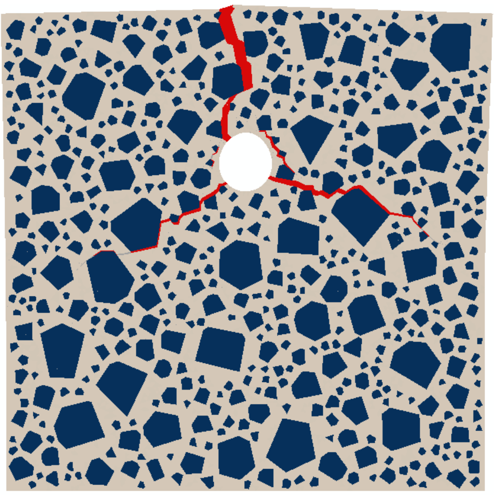

(a) T_0=0, $\eta = 0.26\%$

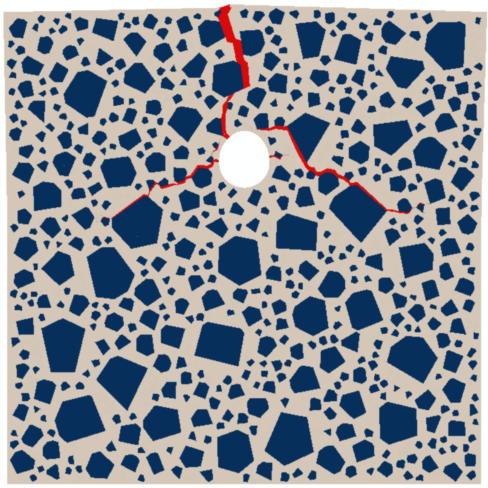

(b) T_0=12.5 μm, $\eta = 0.26\%$

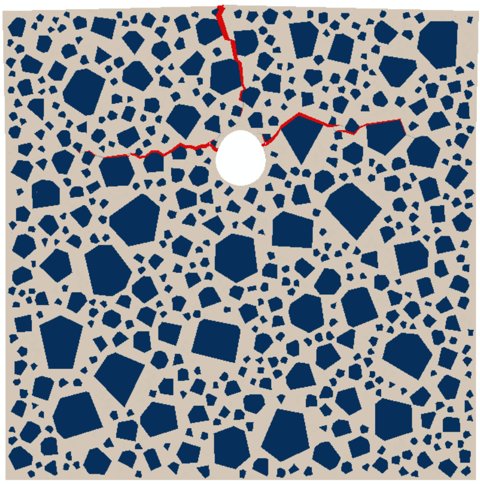

(c) T_0=25 μm, $\eta = 0.26\%$

Figure 18 Effect of the thickness of "porous zone" on crack pattern for non-uniform corrosion coefficient k=2

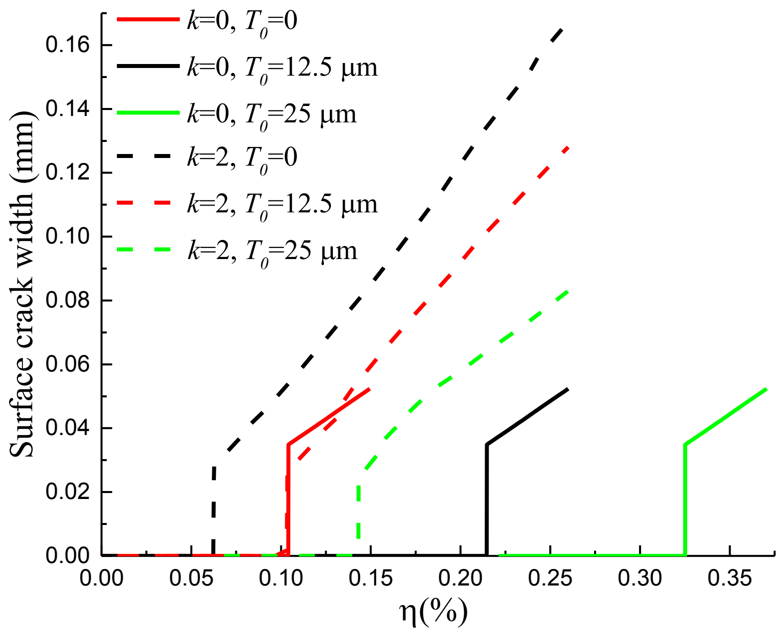

Figure 19 Effect of the thickness of "porous zone" on the evolution of surface crack width